

# CA-UDA: Class-Aware Unsupervised Domain Adaptation with Optimal Assignment and Pseudo-Label Refinement

Can Zhang  
National University of Singapore  
can.zhang@u.nus.edu

Gim Hee Lee  
National University of Singapore  
dcs1gh@nus.edu.sg

## Abstract

Recent works on unsupervised domain adaptation (UDA) focus on the selection of good pseudo-labels as surrogates for the missing labels in the target data. However, source domain bias that deteriorates the pseudo-labels can still exist since the shared network of the source and target domains are typically used for the pseudo-label selections. The suboptimal feature space source-to-target domain alignment can also result in unsatisfactory performance. In this paper, we propose CA-UDA to improve the quality of the pseudo-labels and UDA results with optimal assignment, a pseudo-label refinement strategy and class-aware domain alignment. We use an auxiliary network to mitigate the source domain bias for pseudo-label refinement. Our intuition is that the underlying semantics in the target domain can be fully exploited to help refine the pseudo-labels that are inferred from the source features under domain shift. Furthermore, our optimal assignment can optimally align features in the source-to-target domains and our class-aware domain alignment can simultaneously close the domain gap while preserving the classification decision boundaries. Extensive experiments on several benchmark datasets show that our method can achieve state-of-the-art performance in the image classification task.

## 1. Introduction

Domain shift [41] refers to the phenomenon where the distribution between two data for a closely related task differs significantly. Despite the success of deep learning in many computer vision-related tasks [14, 39, 16, 21], domain shift can cause a deep network to fail catastrophically when it is trained and used on data for the same task but from different distributions. A naive approach is to augment training data across different domains [4, 12, 43], but unfortunately, this approach quickly becomes impractical due to the expensive cost and laborious effort incurred to label large amounts of training data. Unsupervised domain

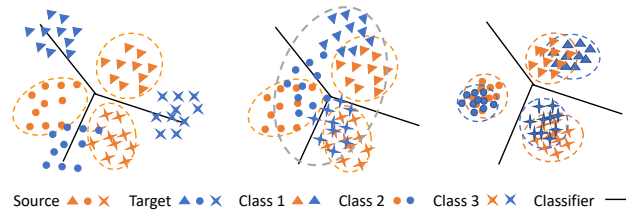


Figure 1. (Best viewed in color.) Illustration of UDA. (Left) Source-only learning from labeled source data, and (Middle) global alignment that matches marginal data distribution across domains without class information lead to poor classification results on the target data. (Right) Our class-aware alignment reduces conditional distribution discrepancy.

adaptation (UDA) is a more pragmatic alternative, where the goal is to transfer task-specific knowledge, e.g. image classification, from a labeled source domain to an unlabeled target domain. The solution to this challenging problem can potentially be used in many practical applications such as self-driving cars, augmented/virtual reality, etc; where the labeled source data can be collected in a controlled laboratory environment, e.g. simulations, while the unlabeled target data is from a closer-to-deployment environment, e.g. parking garages and highways.

Over the years, many works [10, 26, 43, 8, 20] have been proposed to solve the UDA problem by learning domain-invariant feature representations using a shared feature extractor to align the source and target domains. These works are largely inspired by the theoretical results from [2, 28, 29], which state that the target error is bounded by the source error and the divergence between marginal distributions in source and target domains. Consequently, these domain-invariant feature learning works aim to minimize the source error and the source-target discrepancy via task-specific and distribution alignment losses. However, some of these works focus on aligning domain-level distributions without too much consideration on the categorical information in the target domain. As illustrated in Figure 1 (Middle), this leads to incorrect predictions of the classes in the

target domain near the class decision boundaries.

In view of the challenge in the missing categorical information from the target domain, many recent works on UDA have proposed the use of pseudo-labels as surrogates. Several works [20, 32, 35] directly use target domain outputs generated from the network trained by the source domain as pseudo-labels. These target domain pseudo-labels are then used together with the source domain ground truth labels to provide class-level supervision to the network while minimizing the domain discrepancy loss. However, as mentioned in [7], the learned classifier on source domain data might not be able to accurately predict the target samples when the domain shift is large. The accumulated errors from the erroneous pseudo-labels eventually lead to unsatisfactory results. Other works proposed the use of classification confidence [7, 44, 8] to select good pseudo-labels for training. Although these works have shown better results with their pseudo-label selection strategies, source domain bias can still exist since the pseudo-label selections are done with the shared network of the source and target domains. This consequently limits the accuracy of the pseudo-labels, especially in the presence of a large domain shift. Furthermore, the greedy nearest-neighbor feature space source-to-target domain alignment strategy used by most existing works [7, 37, 44, 8] can lead to: 1) suboptimal alignment in the feature space, and 2) poor alignment in the output classification space.

In this paper, we propose CA-UDA to solve the UDA problem. Our CA-UDA improves the quality of the pseudo-labels in the target domain with a **pseudo-label refinement** strategy. We train an *auxiliary network* on the pseudo-labeled target samples with the easy-to-hard learning strategy. The source domain bias is mitigated since the auxiliary network is trained only on the target domain. Our intuition is that the underlying semantics in the target domain can be fully exploited to help refine the pseudo-labels that are inferred from the source features under domain shift. We then select easy samples with confidences higher than a threshold. The confidence is predicted by the optimized target-specific network to avoid domain bias from the source data. In addition, we introduce an **optimal assignment** step to optimally align the features of the source and target domains, and a **class-aware domain alignment** to simultaneously close the domain gap while preserving the classification decision boundaries using an inter-cluster and intra-cluster loss in feature and label space.

Our contributions are summarized as follows:

- We formulate a novel pseudo-label estimation and refinement procedure for UDA using optimal assignment and a self-paced easy-to-hard learning strategy.
- We introduce a cross-domain center-to-center inter-cluster and an in-domain probability-to-probability

intra-cluster loss to jointly minimize the class-aware discrepancy across domains (Figure 1 (Right)).

- Our method achieves the state-of-the-art performance on 4 benchmark datasets in the classification tasks.

## 2. Related Work

The work [2] theoretically proves that the minimization of marginal distribution discrepancy between the source and target domains can help reduce the error in target label estimation. This work established the foundation for many subsequent works on UDA [11, 26, 43, 38]. Several works [11, 33, 10] adopt adversarial training to learn domain-invariant feature representations. DANN [11] leverages a gradient reversal layer to reduce the domain gap in feature space. ADDA [43] utilizes domain discriminator to adversarially learn the target encoder. Other works minimize distribution divergence to align the data. These methods include: maximum mean discrepancy (MMD) in [26] and correlation alignment (CORAL) in [40]. However, these methods only align domain-level distribution. Target samples that lie near margins of the clusters or far from their corresponding class centroids are still susceptible to mis-classification. In contrast, our method is designed to mitigate the class-conditioned distribution shift by class-aware domain alignment.

In the more recent works, pseudo-labels are used as surrogates for the missing labels in the target domain. Several methods [44, 32, 25, 8, 7] formulate class-conditioned domain alignment by minimizing the distribution discrepancy of the prototypes. TPN [32] assigns pseudo-labels to the target samples by their nearest source prototypes and then aligns prototypical distributions. CAN [20] proposes a novel metric to model the class-level distribution discrepancy. However, these methods directly use pseudo-labels as supervision to optimize network parameters. Wrong labels can hinder the class-aware domain alignment performance. To alleviate the wrong label problem, the semantic transfer network [44] employs an alignment loss on centroids. [7] integrates the network with an easy-to-hard strategy to progressively select easy samples for domain alignment. Some works [37, 46] adopt self-training by iteratively predicting pseudo-labels from the network and re-training the network with these labels. However, these methods generate pseudo-labels by the model trained on the source data. Consequently, the source domain bias that remains can deteriorate the quality of the pseudo-labels. In our work, we additionally introduce an optimal assignment step to reduce noises in the pseudo-labels and a pseudo-label refinement step to improve the quality of the pseudo-labels and their confidence. The experimental results empirically show the effectiveness of our approach.

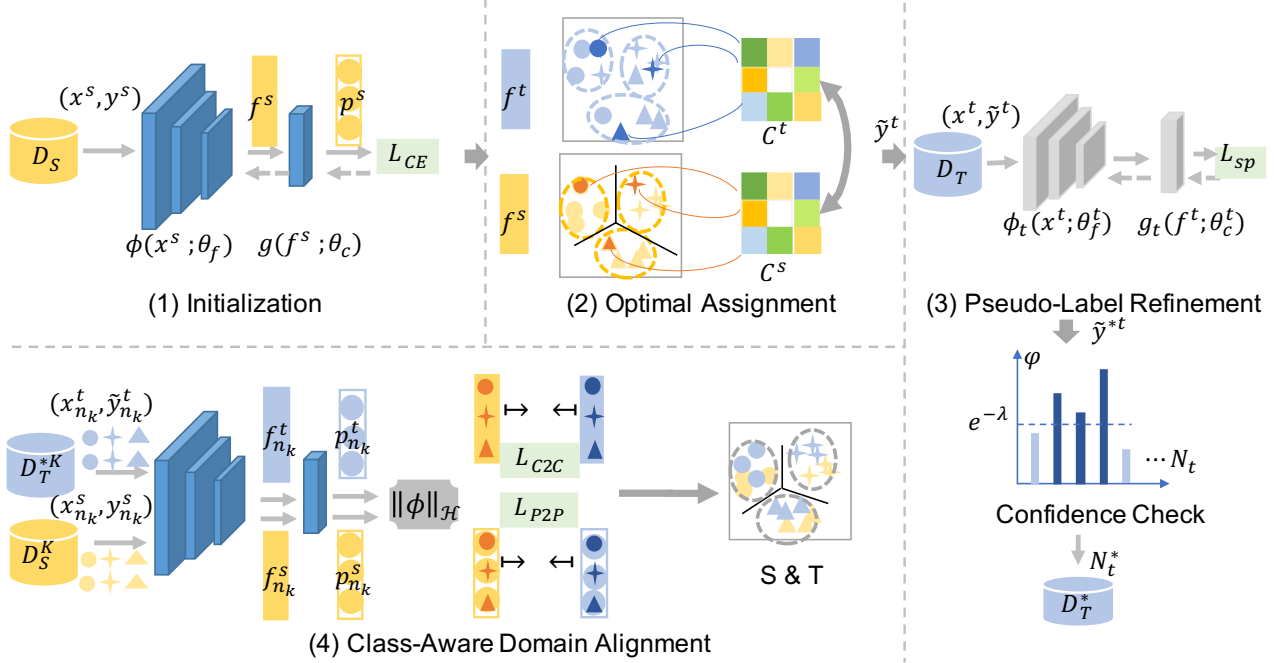


Figure 2. The overall framework of CA-UDA with four steps. 1) The network is pre-trained with the labeled source data  $D_S$ . 2) Do clustering on the target feature embeddings  $f^t$  to obtain cluster centroids  $C^t$ , and then perform the optimal assignment to generate pseudo-labels  $\tilde{y}^t$  with source cluster centroids  $C^s$ . 3) An auxiliary network  $g_t(\phi_t(x^t; \theta_f^t); \theta_c^t)$  is trained by an easy-to-hard refinement loss  $\mathcal{L}_{sp}$  to alleviate wrong pseudo-labels. A confidence check step is introduced to construct new target set  $D_T^*$  with  $N_t^*$  reliable samples that satisfy the condition  $\varphi(x^t, \tilde{y}^t) \geq e^{-\lambda}$ . 4) We do class-aware sampling and then enforce two novel losses, i.e.  $\mathcal{L}_{C2C}$  and  $\mathcal{L}_{P2P}$ , in feature and label space to jointly align class-conditioned distribution. Step 2 to 4 are alternated in every iteration during optimization.

### 3. Problem Formulation

UDA aims to deal with the domain shift problem between labeled source data  $D_S = \{(x_i^s, y_i^s)\}_{i=1}^{N_s}$  and unlabeled target data  $D_T = \{x_i^t\}_{i=1}^{N_t}$ . Given  $N_s$  source samples  $D_S$  and  $N_t$  target samples  $D_T$  with the shared label space  $\mathcal{Y}$ , we expect to make prediction  $\{\hat{y}^t\}$  of  $\{x^t\}$  by utilizing the source label information  $\{y^s\}$ , where  $|\mathcal{Y}| = K$  and  $y^s \in \{0, 1, \dots, K-1\}$  represent the label space with  $K$  classes. Based on the assumption from [27, 42], there exists a shared feature space across domains, and the goal is to learn an domain-invariant feature embedding function  $\phi(x; \theta_f) : x \mapsto f$  that maps  $x$  to the shared feature space and a classifier  $g(f; \theta_c) : f \mapsto \mathcal{Y}$  that maps features to the label space.  $\{\theta_f, \theta_c\}$  are the learnable parameters of the network, denoted as a composition function  $g(\phi(x; \theta_f); \theta_c)$ .

### 4. Our Method

Figure 2 shows our CA-UDA framework with four main steps: 1) initialization, 2) optimal assignment, 3) pseudo-label refinement, and 4) class-aware domain alignment.

#### 4.1. Initialization

We initialize our classification network by training with the labeled source domain data  $D_S$ . After training, a set

of feature embeddings  $f^s = \{f_1^s, \dots, f_{N_s}^s\}$  for the labeled source domain data  $D_S$  and  $f^t = \{f_1^t, \dots, f_{N_t}^t\}$  with the corresponding pseudo-labels  $\tilde{y}^t = \{\tilde{y}_1^t, \dots, \tilde{y}_{N_t}^t\}$  for the unlabeled target domain data  $D_T$  are generated, where features with the same class in the same domain are potentially clustered as observed in DeepCluster [6]. Note that we only initialize the network once. In the subsequent training epochs, the target domain feature embeddings  $f^t$  and pseudo-labels  $\tilde{y}^t$ , and the source domain feature embeddings  $f^s$  are directly obtained from the current network.

#### 4.2. Optimal Assignment

The goal of the optimal assignment step is to assign pseudo-labels to the target domain feature embeddings  $f^t$  using  $f^s$  and its corresponding labels  $y^s$ . Due to the lack of strong labels for the target domain data, we apply the unsupervised k-means algorithm [19] on  $f^t$  to get  $K$  clusters  $C^t = \{c_1^t, \dots, c_K^t\}$ , where  $c_k^t$  is the centroid of the  $k^{\text{th}}$  cluster. Intuitively, feature embeddings that belong to the same class should get assigned to the same cluster. Nonetheless, the actual label of each cluster remains unknown at this stage since unsupervised clustering algorithms such as k-means are based on nearest-neighbor.

The optimal assignment is used to circumvent the problem of missing labels in the target feature embedding clus-

ters  $C^t$ . To this end, we first compute the centroids of the feature embeddings  $C^s = \{c_1^s, \dots, c_K^s\}$  in the source domain using the known labels  $y^s$ , where  $c_k^s$  is the centroid of the feature embeddings corresponding to the class label  $k$ . Subsequently, we align two sets of clusters  $C^s$  and  $C^t$  using optimal assignment. Formally, the optimal alignment of the two sets of clusters is formulated as a linear program:

$$\begin{aligned}
& \text{minimize} && \sum_{i \in |C^s|, j \in |C^t|} d_{ij} m_{ij} \\
& \text{subject to} && \sum_{i \in |C^t|} m_{ij} = 1, \quad j \in |C^s| \\
& && \sum_{j \in |C^s|} m_{ij} = 1, \quad i \in |C^t| \\
& && m_{ij} \in \{0, 1\}, \quad i \in |C^s|, j \in |C^t|,
\end{aligned} \tag{1}$$

where  $d_{ij}$  is the Euclidean distance between the  $i^{\text{th}}$  and  $j^{\text{th}}$  centroids in the source  $c_i^s$  and target  $c_j^t$  domains.  $m_{ij} \in \mathbf{M}$  is an element in the  $K \times K$  permutation matrix  $\mathbf{M}$ .  $m_{ij} = 1$  indicates that the cluster  $c_i^s$  from the source domain and  $c_j^t$  from the target domain are assigned as a match. The two summation constraints ensure the uniqueness of the cluster assignment. The objective of the optimal assignment is to find the optimal permutation matrix  $\mathbf{M}$  such that the total distance between all the corresponding cluster pairs are minimized. We use the Hungarian algorithm [22] as solver for the optimal assignment. After the optimal alignment of the clusters, each target cluster in  $C^t$  is pseudo-labeled by the label of its corresponding source cluster and we have pseudo-label set  $\tilde{y}^t = \{\tilde{y}_1^t, \dots, \tilde{y}_{N_t}^t\}$ .

**Remarks:** It should be noted that pseudo-labels  $\tilde{y}^t$  in the target domain are far from ideal at this stage. In particular, these pseudo-labels are noisy and corrupted with outliers, and thus there exists a lot of samples in the target domain with discrepancies between  $\tilde{y}^t$  and true  $y^t$ . These discrepancies are plentiful especially in the decision boundaries due to two reasons: 1) k-means is based on nearest neighbors and does not discriminate against classes; and 2) the classification network trained on the source domain does not work well on the target domain due to domain shift.

### 4.3. Pseudo-Label Refinement

To mitigate the detrimental effects of wrong pseudo-labels, we propose an easy-to-hard pseudo-label refinement process to improve the quality of the pseudo-labels inspired by self-paced learning [23]. An auxiliary classification network  $g_t(\phi_t(x; \theta_f^t); \theta_c^t)$  is trained in the target domain independently, which aims to simultaneously select easy samples and learn network parameters  $\theta^t$ , i.e.  $\theta_f^t$  and  $\theta_c^t$ . According to the definition in [23], easy samples lie far from the decision boundaries and thus their correct labels can be predicted easily. Specifically, we use the following loss

function  $\mathcal{L}_{sp}$  to update the network at the  $n^{\text{th}}$  epoch:

$$\begin{aligned}
& (\theta_{n+1}^t, v_{n+1}) = \arg \min_{\theta^t, v} \mathcal{L}_{sp}(\theta_n^t, v_n), \quad \text{where} \\
& \mathcal{L}_{sp}(\theta_n^t, v_n) = \frac{\mathcal{C}_n^1(\theta_n^t, v_n) + \mathcal{C}_n^2(v_n)}{|x^t|}, \\
& \mathcal{C}_n^1 = \sum_{i=1}^{|x^t|} v_n^i \mathbb{L}(x_i^t, \tilde{y}_i^t; \theta_n^t), \quad \mathcal{C}_n^2 = -\gamma^n \lambda \sum_{i=1}^{|x^t|} v_n^i.
\end{aligned} \tag{2}$$

$\mathbb{L}(\cdot)$  is the negative log-likelihood as in [13] to measure confidence, i.e. the probability of correctness, and  $v_n^i \in \{0, 1\}^{|x^t|}$  is a binary variable to indicate whether the sample  $x_i$  is included for minimization.  $\gamma^n \lambda$  is the confidence threshold at the  $n^{\text{th}}$  epoch to control the target samples to be selected. We initially set the threshold with a low value (i.e.  $\lambda$ ) and gradually increase it by multiplying with a growing factor  $\gamma$ .  $n = \{0, 1, 2, \dots, N_{max}\}$  is the training epoch and  $\gamma$  is a constant. It can be seen that samples with high likelihood  $\varphi = e^{-\mathbb{L}(\cdot)}$  are considered the easy samples and selected with the condition  $\varphi \geq e^{-\gamma^n \lambda}$ . The selection gradually expands to the more difficult samples as  $n$  increases. The parameter update proceeds until the entire target data are used and the maximum epoch is reached, i.e.  $v_n^i = 1, \forall i$  and  $n = N_{max}$ . The optimum parameters  $\theta^{t*}$  are cached for continuous update in the next iteration. To alleviate the wrong pseudo-label problem for domain alignment, we perform a confidence-check step to only select easy samples in  $D_T$ , which satisfy the condition  $\varphi(x_i^t, \tilde{y}_i^t; \theta^{t*}) \geq e^{-\lambda}$ , to construct new target training set  $D_T^* = \{(x_i^t, \tilde{y}_i^t)\}_{i=1}^{N_t^*}$  with  $N_t^*$  samples. Specifically, we set  $n = 0$  for simplicity and use  $\lambda$  as the confidence threshold to filter out hard samples which lie near the decision margins in the target domain.

**Remarks:** In curriculum [3] and self-paced learning [23], it is observed that a deep network overfits quickly to samples with bad labels in training data. It is thus beneficial to first train the network with easier samples, i.e. samples with potentially correct labels, before adding the harder samples. As discussed in the previous section, noisy pseudo-labels still exist from the optimal assignment step. It is therefore necessary to independently train a target-specific network on instances  $x^t$  aiming to decouple domain bias in the obtained pseudo-label predictions. The quality of the entire pseudo-labels can be improved with the easy-to-hard learning scheme. Furthermore, the confidence check helps to eliminate errors from the wrong labels by favoring easy samples with high confidence.

### 4.4. Class-Aware Domain Alignment

**Cross-domain inter-clusters.** Once we get the refined pseudo-labels from the previous step, we do a class-aware domain alignment to close the domain gap while preserving the class information. Under the assumption that the shared

label space follows uniform distribution as in [18], samples conditioned on labels are then drawn in both source and target domains ( $D_S$  and  $D_T^*$ ). To this end, we propose a modified MMD loss on the feature embeddings that considers the multiple means formed by the different clusters of classes. We call this the center-to-center loss, i.e.

$$\begin{aligned} \mathcal{L}_{C2C} &= \frac{1}{K} \sum_{k=1}^K \left\| \frac{1}{N_s^k} \sum_{i=1}^{N_s^k} \phi(x_i^{s,k}) - \frac{1}{N_t^k} \sum_{j=1}^{N_t^k} \phi(x_j^{t,k}) \right\|_{\mathcal{H}}^2 \\ &= \frac{1}{K} \sum_{k=1}^K \left\{ \frac{1}{N_s^{k2}} \sum_{i=1}^{N_s^k} \sum_{j=1}^{N_s^k} \mathcal{K}(\phi(x_i^{s,k}), \phi(x_j^{s,k})) \right. \\ &\quad + \frac{1}{N_t^{k2}} \sum_{i=1}^{N_t^k} \sum_{j=1}^{N_t^k} \mathcal{K}(\phi(x_i^{t,k}), \phi(x_j^{t,k})) \\ &\quad \left. - \frac{2}{N_s^k N_t^k} \sum_{i=1}^{N_s^k} \sum_{j=1}^{N_t^k} \mathcal{K}(\phi(x_i^{s,k}), \phi(x_j^{t,k})) \right\}, \quad (3) \end{aligned}$$

where  $\phi(x_i^{s,k}) \in D_S$  and  $\phi(x_j^{t,k}) \in D_T^*$  are the source and target feature embeddings (omitting  $\theta_f$  from  $\phi(x; \theta_f)$ ) with the  $k^{\text{th}}$  class label, respectively.  $\mathcal{K}(\cdot, \cdot)$  is the radial basis kernel function (RBF) and  $\|\cdot\|_{\mathcal{H}}$  is the reproducing kernel Hilbert space. The inner terms in the first line of Eq. 3 denote the square-difference between the two empirical means from the  $k^{\text{th}}$  class of the source and target domains. Putting the inner terms into the summation over  $K$  classes gives us the square-difference between the empirical means of all corresponding classes in the source and target domains. The minimization of  $\mathcal{L}_{C2C}$  is equivalent to the minimization of the inter-cluster center-to-center distances between the source and target domains. In our experiments, two batches of samples in an epoch:  $B_S = \{(x_i^{s,k}, y_i = k)\}_{i=1}^{N_s^k}$  and  $B_T = \{(x_i^{t,k}, \tilde{y}_i = k)\}_{i=1}^{N_t^k}$  are sampled from  $D_S$  and  $D_T^*$  according to the class label  $k \in \mathcal{Y}_B \subset \mathcal{Y}$ . The mini-batch label space  $\mathcal{Y}_B$  consists of  $K_B$  classes, i.e.  $|\mathcal{Y}_B| = K_B$ . Each class has  $N_s^k$  source and  $N_t^k$  target samples, respectively. The labels in  $\mathcal{Y}_B$  to be aligned are uniformly chosen from the shared label space  $\mathcal{Y}$  to ensure a shared distribution in the corresponding empirical means across domains. Consequently, the class imbalance within the domain and class-distribution shift across domains can be mitigated from the sampling perspective.

**In-domain intra-clusters.** In similar vein, we introduce another probability-to-probability loss on the output probability of the classification layer, i.e.

$$\mathcal{L}_{P2P} = \frac{1}{K} \sum_{k=1}^K \left\| \frac{1}{N_s^k} \sum_{i=1}^{N_s^k} p_i^{s,k} - \frac{1}{N_t^k} \sum_{j=1}^{N_t^k} p_j^{t,k} \right\|_{\mathcal{H}}^2, \quad (4)$$

where  $p_i^{s,k}$  and  $p_j^{t,k}$  are the probabilities of a source  $x_i^s$  and target  $x_j^t$  domain samples taking the  $k^{\text{th}}$  class label, respec-

tively.  $\mathcal{L}_{P2P}$  aims to minimize the probability difference of the source and target samples in the same class. It is important that  $\mathcal{L}_{P2P}$  has to be minimized together with the cross-entropy loss  $\mathcal{L}_{CE}(x^s, y^s)$  from the fully supervised source domain. Specifically,  $\mathcal{L}_{CE}(x^s, y^s)$  provides a constraint on the probability values in Eq. 4 that forces the in-domain feature embeddings into more discriminative clusters. This implies that in addition to maximizing the in-domain inter-cluster distances of the feature embeddings, the in-domain intra-cluster distances are concurrently minimized towards shaping a better decision boundary.

## 4.5. Optimization.

The optimization of our classification network for UDA is performed by an initialization step and an alternating three-stage training procedure over last three steps. The first initialization step is only performed once.

**1) Initialization.** We initialize our network by doing a fully supervised pre-training on the labeled source data, where we minimize the cross-entropy loss over the network parameters  $\theta = \{\theta_f, \theta_c\}$ :

$$\mathcal{L}_{CE} = - \mathbb{E}_{(x^s, y^s) \sim D_S} \sum_{k=1}^K \mathbb{1}_{c=y^s} \log(y|x^s). \quad (5)$$

**2) Optimal assignment.** At the start of every training iteration, the k-means and optimal assignment are performed, where the initial centroids of the k-means on the unlabeled target domain data are generated from the the labeled source cluster centroids. Subsequently, we cache the centroids from the previous epoch into the memory and update them by a simple moving average in the current epoch:

$$c_k \leftarrow \frac{\phi_k(x; \theta_f)}{\|\phi_k(x; \theta_f)\|_2} + \alpha \cdot c_k, \quad (6)$$

to ensure stability and efficiency.  $\alpha$  is the update momentum coefficient set to 1 for simplicity.  $\phi_k(x; \theta_f)$  is the feature embedding assigned to the  $k^{\text{th}}$  cluster from the nearest neighbor search. We use the Hungarian algorithm [22] as the solver for the optimal assignment problem formulated as a linear program in Eq. 1.

**3) Pseudo-label refinement.** Parameters  $\theta_f^t$  and  $\theta_c^t$  of the auxiliary network  $g_t(\phi_t(x; \theta_f^t); \theta_c^t)$  are updated based on the pseudo-labels obtained from the previous optimal assignment step. The easy-to-hard refinement loss  $\mathcal{L}_{sp}$  from Eq. 2 is iteratively minimized by gradually increasing the threshold  $\gamma^n \lambda$  with the iterations, until all target samples are included and the maximum epoch is reached. The optimum parameters  $\theta^{t*}$  are cached for continuous optimization in the next iteration. Finally, the confidence check selects reliable examples that pass the confidence threshold  $\lambda$  to construct a new training target set  $D_T^* = \{(x_i^t, \tilde{y}_i^t)\}_{i=1}^{N_t^*}$ , i.e.  $e^{-\mathbb{L}(x_i^t, \tilde{y}_i^t; \theta^{t*})} \geq e^{-\lambda}$ .

**4) Class-aware domain alignment.** For training efficiency, we uniformly sample a subset classes from which  $n$  samples are randomly drawn in the source and target domain, i.e.  $x^k = \{x_1^k, \dots, x_n^k\}$ ,  $\forall K$ , where  $x_n^k \sim (D_S^k, D_T^k)$ . The total loss  $\mathcal{L}_{DA}$  we used to train the classification network  $g(\phi(x; \theta_f); \theta_c)$  consists of the center-to-center  $\mathcal{L}_{C2C}$  (cf. Eq. 3), probability-to-probability  $\mathcal{L}_{P2P}$  (cf. Eq. 4), and source domain cross-entropy  $\mathcal{L}_{CE}(x^s, y^s)$  loss terms:

$$\mathcal{L}_{DA} = \mathbb{E}_{x^1, \dots, x^K} \{ \tau_1 \mathcal{L}_{C2C} + \tau_2 \mathcal{L}_{P2P} + \mathcal{L}_{CE}(x^s, y^s) \}, \quad (7)$$

where  $\tau_1$  and  $\tau_2$  are hyperparameters to balance the losses.

## 5. Experiments

We conduct experiments on four standard benchmark datasets: 1) Office-31 [36], 2) ImageCLEF-DA [1], 3) VisDA-2017 [34] and 4) Digit-Five to evaluate the performance of our proposed CA-UDA framework in comparison to other existing state-of-the-art methods. In addition, we show ablation studies to evaluate the effectiveness of each component in our framework.

### 5.1. Datasets and Experimental Setting

**Datasets.** **Office-31** [36] includes three domains: Amazon (A), DSLR (D) and Webcam (W), and contains a total of 4,110 images covering 31 categories. A combination of six pairs of source-target domain settings are evaluated. **ImageCLEF-DA** [1] includes three domains: Caltech-256 (C), ImageNet ILSVRC 2012 (I), and Pascal VOC 2012 (P) with 12 categories, where each category contains equal number of 50 images. **VisDA-2017** [34] is a challenging dataset due to the big domain shift between the synthetic images (152,397 images from VisDA) and the real images (55,388 images from COCO). We evaluate our method on the setting of synthetic-to-real as the source-to-target domain. To make a fair comparison with other methods, We choose the following three digit datasets: MNIST (M) [24], USPS (U) [9] and SVHN (S) [31] in **Digit-Five** as different domains. MNIST (M) and USPS (U) are handwritten Digits containing 70K and 9.3K images, respectively. SVHN has 100K colored digits collected from the real world.

**Implementation details.** For object classification datasets, we adopt ResNet-50 [14] and Resnet-101 [15] pretrained on the ImageNet as the backbone. The last FC layer is replaced with one FC layer of task-specific dimensions. The network parameters are all shared between source and target domain except for the batch normalization layers. We fine-tune the network feature extractor and train the classifier from scratch. For digit classification, we follow the network architecture in [10] and [5], where there are only two convolutional layers as the feature extractor. We use stochastic gradient descent

(SGD) with momentum of 0.9 and weight decay of 0.0005 to train the network. We set the learning rate schedule  $\eta_p = \frac{\eta_0}{(1+\alpha t)^\beta}$  as in [10, 11, 20, 27, 33, 43]. Specifically, the iteration  $t$  linearly changing from 0 to 1,  $\alpha = 10$  &  $\beta = 0.75$ . Following [20, 43],  $\beta = 2.25$  for VisDA-2017 dataset,  $\eta_0 = 0.001$  for feature extractor,  $\eta_0 = 0.01$  for task-specific classifier. We empirically set the hyperparameters in Eq. 2 to  $\lambda = 0.1, \gamma = 1.3$ . This corresponds to the initial likelihood  $e^{-\lambda} \simeq 0.9$  that decreases with an exponential decay  $(\cdot)^\gamma$ . For  $\tau_1$  and  $\tau_2$  in Eq. 7, a sensitively analysis is done on VisDA-2017, and the best performing  $\tau_1 = \tau_2 = 0.3$  is obtained.

**Baselines.** We compare our CA-UDA with several baselines to verify its effectiveness: 1) **Source-only**. 2) Domain-level alignment methods. Representative baselines include: discrepancy-based models, i.e. **DAN** [26] and **JAN** [27], and adversarial-discriminative models, i.e. **DANN** [11], **MADA** [33], **MCD** [38] and **RevGrad** [10]. 3) Class conditional alignment methods which utilize pseudo-labels as supervision in the target domain, i.e. **TPN** [32], **CAN** [20] and **A<sup>2</sup>LP** [45], and several baselines that also consider to solve the wrong pseudo-label problem, i.e. **CAT** [8], **MSTN** [44] and **PFAN** [7].

### 5.2. Comparison with Baselines

**Digit classification.** We evaluate our CA-UDA framework on three source-to-target domain adaptation settings from the Digit-Five dataset:  $M \rightarrow U$ ,  $U \rightarrow M$  and  $S \rightarrow M$ . Table 1 shows that our method achieves state-of-the-art performance in all three domain adaptation subtasks. Compared with DAN [26] and JAN [27], class-level alignment methods generally perform much better. It indicates that matching distribution for each category helps to improve domain alignment. In comparison to TPN that uses prototype alignment, our CA-UDA is observed to achieve higher accuracy, e.g. in  $S \rightarrow M$ , our CA-UDA achieves +4.63% and +5.49% with  $\mathcal{L}_{sp}$ . It implies the effectiveness of the optimal assignment and pseudo-label refinement in our CA-UDA in reducing the negative effects from wrong pseudo-labels. Furthermore, our model outperforms or shows comparable performance with the pseudo-labeling baselines. This confirms the capability of our proposals for mitigating domain shift in pseudo-label predictions.

**Object classification.** We further evaluate our CA-UDA on the object classification datasets. Table 2 evidently shows the improved accuracy over the six transfer directions across three domains on **Office-31**. Compared to A<sup>2</sup>LP [45], our CA-UDA with  $\mathcal{L}_{sp}$  boosts performance by 7.45% and 7.24% in  $W \rightarrow A$  (85.05%) and  $D \rightarrow A$  (85.34%), respectively. These results highlight the advantage of our pseudo-label refinement step, which improves the quality of pseudo-labels in the target domain for bet-

Method	M → U	U → M	S → M	mean
Source-only	75.2	57.1	60.1	64.1
RevGrad [10]	77.1	73.0	73.9	74.7
DAN [26]	80.3	77.8	73.5	77.2
JAN [27]	84.4	83.4	78.4	82.1
MCD [38]	90.0	88.5	83.3	87.3
DANN [11]	90.4	94.7	84.2	89.8
TPN [32]	92.1	94.1	93.0	93.1
MSTN [44]	92.9	-	91.7	-
PFAN [7]	95.0	-	93.9	-
rRevGrad+CAT [8]	94.0	96.0	<b>98.8</b>	96.27
Ours (without $\mathcal{L}_{sp}$ )	93.79	96.62	97.63	96.01
Ours (with $\mathcal{L}_{sp}$ )	<b>95.43</b>	<b>97.22</b>	98.49	<b>97.05</b>

Table 1. Classification accuracy (%) on Digit-five.

Method	A → W	W → A	A → D	D → A	W → D	D → W	mean
Source-only	68.4	60.7	68.9	62.5	99.3	96.7	76.1
RevGrad [10]	82.0	67.4	79.7	68.2	99.1	96.9	82.2
DAN [26]	80.5	62.8	78.6	63.6	99.6	97.1	80.4
JAN [27]	85.4	70.0	84.7	68.6	99.8	97.4	84.3
MADA [33]	90.0	66.4	87.8	70.3	99.6	97.4	85.3
MSTN [44]	91.3	65.6	90.4	72.7	100.0	98.9	86.5
rRevGrad+CAT [8]	94.4	70.2	90.8	72.2	100.0	98.0	87.6
CAN [20]	94.5	77.0	95.0	78.0	99.8	99.1	90.6
A <sup>2</sup> LP [45]	93.4	77.6	96.1	78.1	<b>100</b>	98.8	90.7
Ours (without $\mathcal{L}_{sp}$ )	93.96	77.21	93.37	78.31	<b>100</b>	98.36	90.20
Ours (with $\mathcal{L}_{sp}$ )	<b>96.23</b>	<b>85.05</b>	<b>98.19</b>	<b>85.34</b>	<b>100</b>	<b>99.25</b>	<b>94.01</b>

Table 2. Accuracy (%) on Office-31 (ResNet-50).

Method	I → P	P → I	I → C	C → I	C → P	P → C	mean
Source-only	74.8	83.9	91.5	78	65.5	91.2	80.8
DAN [26]	74.5	82.2	92.8	86.3	69.2	89.8	82.5
DANN [11]	75.0	86.0	96.2	87.0	74.3	91.5	85.0
JAN [27]	76.8	88.0	94.7	89.5	74.2	91.7	85.8
rRevGrad+CAT [8]	77.2	91.0	95.5	91.3	75.3	93.6	87.3
A <sup>2</sup> LP [45]	79.8	94.3	97.7	93.0	79.9	96.9	90.3
Ours (without $\mathcal{L}_{sp}$ )	78.67	94.50	98.00	94.00	79.33	97.67	90.36
Ours (with $\mathcal{L}_{sp}$ )	<b>83.50</b>	<b>96.83</b>	<b>98.83</b>	<b>97.17</b>	<b>82.67</b>	<b>99.00</b>	<b>93.00</b>

Table 3. Accuracy (%) on ImageCLEF-DA (ResNet-50).

Method	Acc. (ResNet50)	Acc.(ResNet101)
Source-only	45.6	50.8
DAN [26]	53.0	61.1
DANN [11]	55.0	57.4
MCD [38]	-	71.9
CAN [20]	-	87.2
A <sup>2</sup> LP [45]	86.5	87.6
Ours (without $\mathcal{L}_{sp}$ )	85.45	86.44
Ours (with $\mathcal{L}_{sp}$ )	<b>87.13</b>	<b>88.72</b>

Table 4. Classification accuracy (%) on VisDA-2017.

ter class-aware domain alignment. Although this dataset has class imbalance within each domain and in-class data imbalance across domains, our CA-UDA still consistently achieves the best performance. We conjecture that it is our class-level sampling that makes our model effective on the imbalanced data.

Table 3 reports results on six adaptation tasks between pairwise domains from **ImageCLEF-DA**. Our CA-UDA with  $\mathcal{L}_{sp}$  significantly outperforms all existing methods on all transfer directions. In contrast to other datasets, the number of samples in each category are identical in all domains. Therefore, the good results reveal the scalability of our CA-

UDA to different datasets.

Table 4 lists the classification accuracy on **VisDA-2017**, where all the baseline results are directly taken from [45]. We evaluate CA-UDA with two backbone networks, i.e. ResNet-50 and ResNet-101. CA-UDA with  $\mathcal{L}_{sp}$  outperforms all baselines. Table 5 summarizes the accuracy over 12 categories. Prediction bias towards some classes can be observed as the performing of all baselines fluctuates over different categories. Our method achieves the best performance on most categories and the highest average accuracy.

### 5.3. Ablation Studies

**Effect of the pseudo-label refinement.** To study the role of pseudo-label refinement in our CA-UDA, we remove the auxiliary target classifier (without  $\mathcal{L}_{sp}$ ) as comparison. Table 1, 2, 3, 4, 5 show classification accuracy on all four benchmarks. Ours (with  $\mathcal{L}_{sp}$ ) achieves more impressive improvements, which can be attributed to: 1) the easy-to-hard pseudo-label refinement step by the target-specific classifier, and 2) the confidence-check step by selecting more reliable samples for class-level alignment. It suggests effective pseudo-label refinement can provide substantial benefits to the class-aware domain alignment.

**Domain alignment evaluation.** Table 6 evaluates our class-level domain alignment  $\mathcal{L}_{DA}$  and its two components, i.e.  $\mathcal{L}_{C2C}$  and  $\mathcal{L}_{P2P}$ . The performance is observed to drop when either one is removed. “ $\mathcal{L}_{CE}^{t,pl_h}$ ” and “ $\mathcal{L}_{CE}^{t,pl_s}$ ” denote two replacements of  $\mathcal{L}_{DA}$ , i.e. direct CE loss on pseudo-labels with hard one-hot and soft entropy weights [17], respectively. In contrast, our  $\mathcal{L}_{P2P}$  and  $\mathcal{L}_{C2C}$  based settings greatly outperform CE-based supervisions by using pseudo labels for discrepancy minimization.

To further evaluate  $\mathcal{L}_{P2P}$ , an additional setting is considered, i.e. “ $\mathcal{L}_{C2C} + \mathcal{L}_1$ ” by replacing  $\mathcal{L}_{P2P}$  with the L1-distance  $\mathcal{L}_1$  as in [38]. In Table 6,  $\mathcal{L}_1$  improves slightly over “ $\mathcal{L}_{C2C}$ ” but drops on ImageCLEF-DA. In comparison, our  $\mathcal{L}_{P2P}$  consistently improves the accuracy, particularly by a large margin on VisDA-2017. It implies that our  $\mathcal{L}_{P2P}$  is effective on different datasets even with complex data diversity.

**Effect of the confidence-check strategy.** Table 7 examines our confidence-check strategy on two datasets, i.e. Office-31 and ImageCLEF-DA. “w/o. CF” means we remove the confidence check and directly use the entire pseudo-labeled target data for domain alignment. It can be observed that overall results of “w/o. CF” are inferior to “w. CF”, which demonstrates effectiveness of the confidence-check after the pseudo-label refinement step. The higher accuracy of “w. CF” is due to the reduction of detrimental influence from wrong pseudo-labels as hard examples with low confidence are filtered out.

Method	plane	bcycl	bus	car	horse	knife	mcycl	person	plant	sktbrd	train	truck	mean
Source-only	70.6	51.8	55.8	68.9	77.9	7.6	93.3	34.5	81.1	27.9	88.6	5.6	55.3
DAN [26]	68.1	15.4	76.5	<b>87.0</b>	71.1	48.9	82.3	51.5	88.7	33.2	<b>88.9</b>	42.2	62.8
JAN [27]	75.7	18.7	82.3	86.3	70.2	56.9	80.5	53.8	92.5	32.2	84.5	54.5	65.7
MCD [38]	87.0	60.9	83.7	64.0	88.9	79.6	84.7	76.9	88.6	40.3	83.0	25.8	71.9
TPN [32]	93.7	85.1	69.2	81.6	93.5	61.9	89.3	81.4	93.5	81.6	84.5	49.9	80.4
CAN [20]	97.9	<b>87.2</b>	82.5	74.3	97.8	96.2	90.8	80.7	96.6	<b>96.3</b>	87.5	59.9	87.2
Ours (without $\mathcal{L}_{sp}$ )	97.48	86.96	83.6	76.73	<b>97.48</b>	<b>97.40</b>	89.73	79.75	96.97	94.43	88.60	48.14	86.44
Ours (with $\mathcal{L}_{sp}$ )	<b>97.92</b>	84.14	<b>87.25</b>	81.51	95.97	97.25	<b>92.7</b>	<b>87.65</b>	<b>96.99</b>	94.52	88.29	<b>60.49</b>	<b>88.72</b>

Table 5. Classification accuracy (%) on VisDA-2017 (ResNet-101).

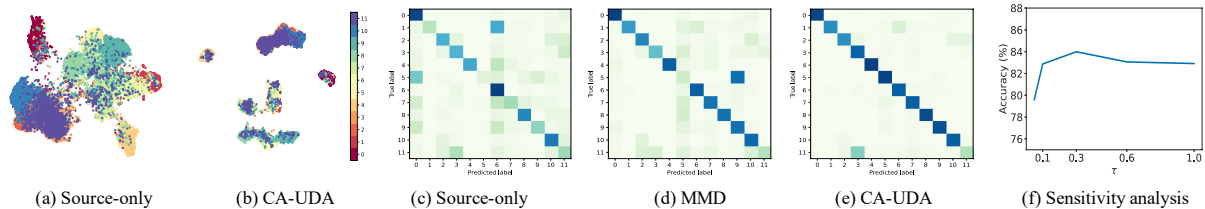


Figure 3. The visualizations of features (a-b) and confusion matrix (c-e) on VisDA-2017 from Source-only, MMD and CA-UDA with  $\mathcal{L}_{sp}$ . 0 to 11 correspond to the order of all categories listed in Table 5. (f) The sensitivity analysis of CA-UDA to  $\tau$ . (ResNet-50)

Dataset	$\mathcal{L}_{CE}^{t,plh}$	$\mathcal{L}_{CE}^{t,pls}$	$\mathcal{L}_{P2P}$	$\mathcal{L}_{C2C}$	$\mathcal{L}_{C2C} + \mathcal{L}_1$ [38]	$\mathcal{L}_{DA}$
Office-31	82.46	84.85	88.15	88.27	89.07	<b>90.20</b>
ImageCLEF-DA	87.42	87.36	89.97	89.83	89.19	<b>90.36</b>

Table 6. Domain alignment evaluation with mean accuracy (%).

Dataset	Net	GMM	Ours(OA)	Ours (w/o. CF)	Ours (w. CF)
Office-31	88.47	89.68	90.20	92.26	<b>94.01</b>
ImageCLEF-DA	89.53	89.92	90.36	91.30	<b>93.00</b>

Table 7. Confidence-check and Pseudo-label generation evaluation with mean accuracy (%).

**Pseudo-label generation evaluation.** Table 7 evaluates the quality of pseudo-labels generated by different approaches in our UDA task: 1) “Net” by predictions from the network, 2) “GMM” by estimations from the Gaussian Mixture Model, 3) “Ours(OA)” by our cluster-based optimal assignment, and “Ours(w/o. CF)” by additionally using pseudo-label refinement without data selection for alignment. All comparisons are conducted under the same setting that adopts  $\mathcal{L}_{DA}$  on the entire data for domain alignment on Office-31 and ImageCLEF-DA. It is observed that our model can generate better pseudo labels by using optimal assignment and our pseudo-label refinement by training a task-specific network is effective in suppressing wrong pseudo-labeled samples for better domain alignment.

#### 5.4. Qualitative Results and Analysis

**Visualization.** Figure 3 (a-e) shows visualizations of different models: 1) Source-only, 2) global alignment based MMD and 3) CA-UDA with  $\mathcal{L}_{sp}$  on the VisDA-2017 dataset. Visualization of target features are done by the umap [30]. Compared with MMD, our CA-UDA shows more compact intra-clusters, more apparent inter-cluster

margins, and also less wrong labels. As visualized by the confusion matrix, a majority of the samples in some categories exhibit confusions for Source-only and MMD, while our CA-UDA significantly alleviates the class conditional shift.

**Sensitivity analysis.** Figure 3 (f) studies the sensitivity of  $\tau_1$  and  $\tau_2$  in Eq. 7 on VisDA-2017, which are balance weights of  $\mathcal{L}_{C2C}$  and  $\mathcal{L}_{P2P}$ . For general analysis, we set  $\tau_1 = \tau_2$  and change the values over the range  $\{0.05, 0.1, 0.3, 0.6, 1.0\}$ . It can be observed that the accuracy curve is bell-shaped, where the performance steadily increases and then starts decreasing from 0.3. We set the best performing  $\tau_1 = \tau_2 = 0.3$  in all experiments.

## 6. Conclusion

In this paper, we propose CA-UDA to improve the quality of the pseudo-labels and UDA results with optimal assignment, a pseudo-label refinement strategy and class-aware domain alignment. In the pseudo-label refinement strategy, we show that the source domain bias in pseudo-label generation can be mitigated with the use of an auxiliary network trained on the target domain data. We further demonstrate that our optimal assignment can optimally align features in the source-to-target domains and our class-aware domain alignment can simultaneously close the domain gap while preserving the classification decision boundaries. Extensive experiments on several benchmark datasets show that our method can achieve state-of-the-art performance in the image classification tasks.

## References

- [1] <https://www.imageclef.org/2014/adaptation/>. 6
- [2] Shai Ben-David, John Blitzer, Koby Crammer, Alex Kulesza, Fernando Pereira, and Jennifer Wortman Vaughan. A theory of learning from different domains. *Machine Learning*, 79(1-2):151–175, 2010. 1, 2
- [3] Yoshua Bengio, Jérôme Louradour, Ronan Collobert, and Jason Weston. Curriculum learning. In *Proceedings of the 26th annual international conference on machine learning*, pages 41–48, 2009. 4
- [4] John Blitzer, Ryan McDonald, and Fernando Pereira. Domain adaptation with structural correspondence learning. In *Proceedings of the 2006 conference on empirical methods in natural language processing*, pages 120–128, 2006. 1
- [5] Konstantinos Bousmalis, Nathan Silberman, David Dohan, Dumitru Erhan, and Dilip Krishnan. Unsupervised pixel-level domain adaptation with generative adversarial networks. In *Proceedings of the IEEE conference on computer vision and pattern recognition*, pages 3722–3731, 2017. 6
- [6] Mathilde Caron, Piotr Bojanowski, Armand Joulin, and Matthijs Douze. Deep clustering for unsupervised learning of visual features. In *Proceedings of the European Conference on Computer Vision (ECCV)*, pages 132–149, 2018. 3
- [7] Chaoqi Chen, Weiping Xie, Wenbing Huang, Yu Rong, Xinghao Ding, Yue Huang, Tingyang Xu, and Junzhou Huang. Progressive feature alignment for unsupervised domain adaptation. In *Proceedings of the IEEE/CVF Conference on Computer Vision and Pattern Recognition*, pages 627–636, 2019. 2, 6, 7
- [8] Zhijie Deng, Yucen Luo, and Jun Zhu. Cluster alignment with a teacher for unsupervised domain adaptation. In *Proceedings of the IEEE International Conference on Computer Vision*, pages 9944–9953, 2019. 1, 2, 6, 7
- [9] Jerome Friedman, Trevor Hastie, and Robert Tibshirani. *The elements of statistical learning*, volume 1. Springer series in statistics New York, 2001. 6
- [10] Yaroslav Ganin and Victor Lempitsky. Unsupervised domain adaptation by backpropagation. In *International conference on machine learning*, pages 1180–1189. PMLR, 2015. 1, 2, 6, 7
- [11] Yaroslav Ganin, Evgeniya Ustinova, Hana Ajakan, Pascal Germain, Hugo Larochelle, François Laviolette, Mario Marchand, and Victor Lempitsky. Domain-adversarial training of neural networks. *The Journal of Machine Learning Research*, 17(1):2096–2030, 2016. 2, 6, 7
- [12] Boqing Gong, Yuan Shi, Fei Sha, and Kristen Grauman. Geodesic flow kernel for unsupervised domain adaptation. In *2012 IEEE Conference on Computer Vision and Pattern Recognition*, pages 2066–2073. IEEE, 2012. 1
- [13] Chuan Guo, Geoff Pleiss, Yu Sun, and Kilian Q Weinberger. On calibration of modern neural networks. In *International Conference on Machine Learning*, pages 1321–1330. PMLR, 2017. 4
- [14] Kaiming He, Xiangyu Zhang, Shaoqing Ren, and Jian Sun. Deep residual learning for image recognition. In *Proceedings of the IEEE conference on computer vision and pattern recognition*, pages 770–778, 2016. 1, 6
- [15] Kaiming He, Xiangyu Zhang, Shaoqing Ren, and Jian Sun. Identity mappings in deep residual networks. In *European conference on computer vision*, pages 630–645. Springer, 2016. 6
- [16] Gao Huang, Zhuang Liu, Laurens Van Der Maaten, and Kilian Q Weinberger. Densely connected convolutional networks. In *Proceedings of the IEEE conference on computer vision and pattern recognition*, pages 4700–4708, 2017. 1
- [17] Ahmet Iscen, Giorgos Tolias, Yannis Avrithis, and Ondrej Chum. Label propagation for deep semi-supervised learning. In *Proceedings of the IEEE conference on computer vision and pattern recognition*, pages 5070–5079, 2019. 7
- [18] Xiang Jiang, Qicheng Lao, Stan Matwin, and Mohammad Havaei. Implicit class-conditioned domain alignment for unsupervised domain adaptation. In *International Conference on Machine Learning*, pages 4816–4827. PMLR, 2020. 5
- [19] Xin Jin and Jiawei Han. *K-Means Clustering*, pages 563–564. Springer US, Boston, MA, 2010. 3
- [20] Guoliang Kang, Lu Jiang, Yi Yang, and Alexander G Hauptmann. Contrastive adaptation network for unsupervised domain adaptation. In *Proceedings of the IEEE Conference on Computer Vision and Pattern Recognition*, pages 4893–4902, 2019. 1, 2, 6, 7, 8
- [21] Alex Krizhevsky, Ilya Sutskever, and Geoffrey E Hinton. Imagenet classification with deep convolutional neural networks. In *NIPS*, 2012. 1
- [22] H. W. Kuhn and Bryn Yaw. The hungarian method for the assignment problem. *Naval Res. Logist. Quart.*, pages 83–97, 1955. 4, 5
- [23] M Pawan Kumar, Benjamin Packer, and Daphne Koller. Self-paced learning for latent variable models. In *Advances in neural information processing systems*, pages 1189–1197, 2010. 4
- [24] Yann LeCun, Léon Bottou, Yoshua Bengio, and Patrick Haffner. Gradient-based learning applied to document recognition. *Proceedings of the IEEE*, 86(11):2278–2324, 1998. 6
- [25] Jian Liang, Ran He, Zhenan Sun, and Tieniu Tan. Distant supervised centroid shift: A simple and efficient approach to visual domain adaptation. In *Proceedings of the IEEE/CVF Conference on Computer Vision and Pattern Recognition*, pages 2975–2984, 2019. 2
- [26] Mingsheng Long, Yue Cao, Jianmin Wang, and Michael Jordan. Learning transferable features with deep adaptation networks. In *International conference on machine learning*, pages 97–105. PMLR, 2015. 1, 2, 6, 7, 8
- [27] Mingsheng Long, Han Zhu, Jianmin Wang, and Michael I Jordan. Deep transfer learning with joint adaptation networks. In *International conference on machine learning*, pages 2208–2217. PMLR, 2017. 3, 6, 7, 8
- [28] Yishay Mansour, Mehryar Mohri, and Afshin Rostamizadeh. Domain adaptation: Learning bounds and algorithms. *arXiv preprint arXiv:0902.3430*, 2009. 1
- [29] Yishay Mansour and Mariano Schain. Robust domain adaptation. *Annals of Mathematics and Artificial Intelligence*, 71(4):365–380, 2014. 1

- [30] Leland McInnes, John Healy, and James Melville. Umap: Uniform manifold approximation and projection for dimension reduction. *arXiv preprint arXiv:1802.03426*, 2018. 8
- [31] Yuval Netzer, Tao Wang, Adam Coates, Alessandro Bisacco, Bo Wu, and Andrew Y. Ng. Reading digits in natural images with unsupervised feature learning. In *NIPS Workshop on Deep Learning and Unsupervised Feature Learning 2011*, 2011. 6
- [32] Yingwei Pan, Ting Yao, Yehao Li, Yu Wang, Chong-Wah Ngo, and Tao Mei. Transferrable prototypical networks for unsupervised domain adaptation. In *Proceedings of the IEEE Conference on Computer Vision and Pattern Recognition*, pages 2239–2247, 2019. 2, 6, 7, 8
- [33] Zhongyi Pei, Zhangjie Cao, Mingsheng Long, and Jianmin Wang. Multi-adversarial domain adaptation. *arXiv preprint arXiv:1809.02176*, 2018. 2, 6, 7
- [34] Xingchao Peng, Ben Usman, Neela Kaushik, Judy Hoffman, Dequan Wang, and Kate Saenko. Visda: The visual domain adaptation challenge. *arXiv preprint arXiv:1710.06924*, 2017. 6
- [35] Pedro O Pinheiro. Unsupervised domain adaptation with similarity learning. In *Proceedings of the IEEE Conference on Computer Vision and Pattern Recognition*, pages 8004–8013, 2018. 2
- [36] Kate Saenko, Brian Kulis, Mario Fritz, and Trevor Darrell. Adapting visual category models to new domains. In *European conference on computer vision*, pages 213–226. Springer, 2010. 6
- [37] Kuniaki Saito, Yoshitaka Ushiku, and Tatsuya Harada. Asymmetric tri-training for unsupervised domain adaptation. In *International Conference on Machine Learning*, pages 2988–2997. PMLR, 2017. 2
- [38] Kuniaki Saito, Kohei Watanabe, Yoshitaka Ushiku, and Tatsuya Harada. Maximum classifier discrepancy for unsupervised domain adaptation. In *Proceedings of the IEEE Conference on Computer Vision and Pattern Recognition*, pages 3723–3732, 2018. 2, 6, 7, 8
- [39] Karen Simonyan and Andrew Zisserman. Very deep convolutional networks for large-scale image recognition. *arXiv preprint arXiv:1409.1556*, 2014. 1
- [40] Baochen Sun, Jiashi Feng, and Kate Saenko. Return of frustratingly easy domain adaptation. In *Proceedings of the AAAI Conference on Artificial Intelligence*, volume 30, 2016. 2
- [41] Antonio Torralba and Alexei A Efros. Unbiased look at dataset bias. In *Proceedings of the IEEE conference on computer vision and pattern recognition*, pages 1521–1528. IEEE, 2011. 1
- [42] Eric Tzeng, Judy Hoffman, Trevor Darrell, and Kate Saenko. Simultaneous deep transfer across domains and tasks. In *Proceedings of the IEEE International Conference on Computer Vision*, pages 4068–4076, 2015. 3
- [43] Eric Tzeng, Judy Hoffman, Kate Saenko, and Trevor Darrell. Adversarial discriminative domain adaptation. In *Proceedings of the IEEE conference on computer vision and pattern recognition*, pages 7167–7176, 2017. 1, 2, 6
- [44] Shaoan Xie, Zibin Zheng, Liang Chen, and Chuan Chen. Learning semantic representations for unsupervised domain adaptation. In *International Conference on Machine Learning*, pages 5423–5432, 2018. 2, 6, 7
- [45] Yabin Zhang, Bin Deng, Kui Jia, and Lei Zhang. Label propagation with augmented anchors: A simple semi-supervised learning baseline for unsupervised domain adaptation. *arXiv preprint arXiv:2007.07695*, 2020. 6, 7
- [46] Yang Zou, Zhiding Yu, BVK Kumar, and Jinsong Wang. Unsupervised domain adaptation for semantic segmentation via class-balanced self-training. In *Proceedings of the European conference on computer vision (ECCV)*, pages 289–305, 2018. 2